

# Go viral or go broadcast? Characterizing the virality and growth of cascades

Yafei Zhang,<sup>1,2</sup> Lin Wang,<sup>1</sup> Jonathan J. H. Zhu,<sup>2,\*</sup> and Xiaofan Wang<sup>1,3,\*</sup>

<sup>1</sup>Department of Automation, Shanghai Jiao Tong University, Shanghai 200240, China

<sup>2</sup>Department of Media and Communication; School of Data Science,

City University of Hong Kong, Hong Kong S.A.R., China

<sup>3</sup>Department of Automation, Shanghai University, Shanghai 200444, China

Quantifying the virality of cascades is an important question across disciplines such as the transmission of disease, the spread of information and the diffusion of innovations. An appropriate virality metric should be able to disambiguate between a shallow, broadcast-like diffusion process and a deep, multi-generational branching process. Although several valuable works have been dedicated to this field, most of them fail to take the position of the diffusion source into consideration, which makes them fall into the trap of graph isomorphism and would result in imprecise estimation of cascade virality inevitably under certain circumstances.

In this paper, we propose a root-aware approach to quantifying the virality of cascades with proper consideration of the root node in a diffusion tree. With applications on synthetic and empirical cascades, we show the properties and potential utility of the proposed virality measure. Based on preferential attachment mechanisms, we further introduce a model to mimic the growth of cascades. The proposed model enables the interpolation between broadcast and viral spreading during the growth of cascades. Through numerical simulations, we demonstrate the effectiveness of the proposed model in characterizing the virality of growing cascades. Our work contributes to the understanding of cascade virality and growth, and could offer practical implications in a range of policy domains including viral marketing, infectious disease and information diffusion.

## I. INTRODUCTION

Spreading is a ubiquitous process across disciplines. Conceptually, many spreading processes can be viewed as tree-like cascades, including the retweeting or resharing of news in online social networks [1–5], the generated discussion threads in online boards [6–8], the outbreak or transmission of diseases [9–12], and the diffusion of new products or services [13–16]. For instance, in a discussion thread, comments and the reply-to actions between them can be represented as nodes and edges in a rooted tree with the original post acting as the root [8].

In some cases, a single node could directly account for a large proportion of the whole diffusion process, which is a typical characteristic in the media broadcast industry; while in others, diffusion is more likely to be driven by word-of-mouth mechanisms and circulate in a viral way, where each node only accounts for a small fraction of the whole diffusion process [1]. For example, one NBA Christmas game is able to attract millions of views through merely broadcast, but one tweet could reach millions as well through viral spreading.

As the backbone of so many diffusion processes, cascade structure yields a valuable source to learn the extent to which a cascade grows in a broadcast (or breadth-first) or viral (or depth-first) way. From the view of tree traversal, we can simply interpret broadcast cascade as a result of “breadth first search” and viral cascade as a result of “depth first search”. In this regard, there have been several important attempts to quantify the virality of cascades [1–3, 13], where the more viral a cascade

is, the larger this virality quantity would be. However, unlike many other undirected graphs, once the root of a cascade is identified, the direction of its growth or flow is thus determined: from the root node to its descendants (see Fig. 1, (a)-(d)). In other words, rooted cascades are actually directed graphs, rather than undirected graphs.

For example, rooted cascades in Fig. 1 (a)-(d) exhibit distinct structures, but if the root nodes are overlooked, they are deemed as the same structure under graph isomorphism (Fig. 1 (e)). More such examples are illustrated in Fig. 2. For ease of visualization, the directed ties in each rooted cascade are not shown hereafter, as the existence of the root node already implies the direction of the flow. Therefore, it’s anticipated that ignoring the root node and simply regarding cascades as undirected trees would inevitably result in imprecise estimation of the virality of cascades under certain situations.

To remedy this, a root-aware approach is proposed to quantify the virality of cascades in this paper. Specifically, instead of computing the average distance between all pairs of nodes in a cascade tree (which is also termed *Wiener index* or *structural virality* [1]), we calculate the

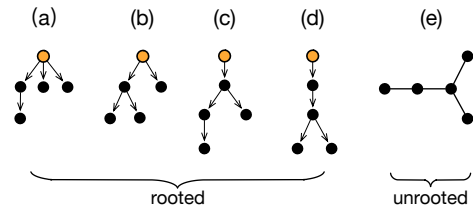


FIG. 1. Examples of rooted cascades and the corresponding unrooted cascade. The root node is colored in orange in each rooted cascade.

\* Corresponding authors

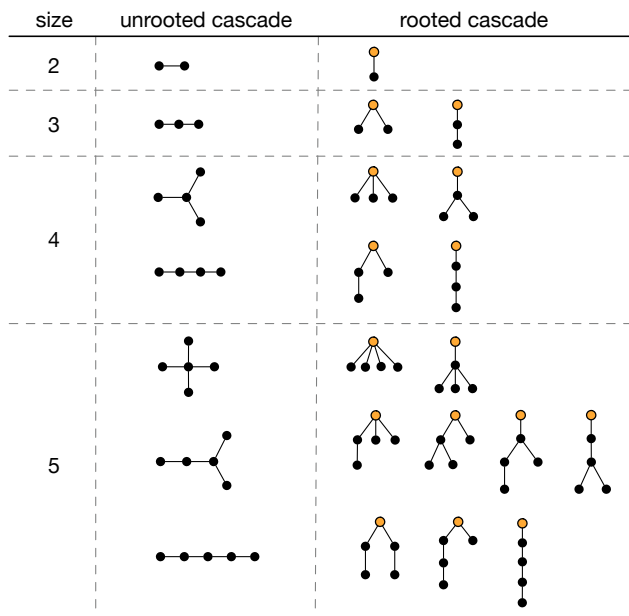


FIG. 2. Unrooted cascades versus the corresponding rooted cascades. For illustration purposes, only cascades of size less than or equal to 5 are shown. The diffusion source is colored in orange in each rooted cascade. For ease of visualization, the directed ties in each rooted cascade are not shown.

average distance between a node and its descendants, and summing the computed distances over all nodes yields the amended virality of a cascade. The proposed approach can operate in a recursive manner, and is able to provide a high-resolution depiction of cascade virality. Leveraging synthetic and empirical cascades, we show the property and potential utility of the quantified cascade virality.

In light of preferential attachment mechanisms [8, 17–22], this work further presents a cascade growth model based on node genealogy instead of merely node degree. Specifically, the genealogy of a given node is defined as the subtree rooted at this node and contains only the given node itself and its descendants, and the probability that a new node attached to an existing node depends on the genealogy size of the target node at different generations. Through numerical simulations, we further demonstrate the benefits brought by genealogy-based modeling (compared with degree-based modeling) in capturing the virality landscape of cascades.

## II. CASCADE VIRALITY

### A. Algorithm

Quantifying the virality of cascades is a challenging task as it synthetically considers not only the size but also the depth and branches of a given cascade tree. Goel et al. [1] address this issue using the *Wiener index*, which

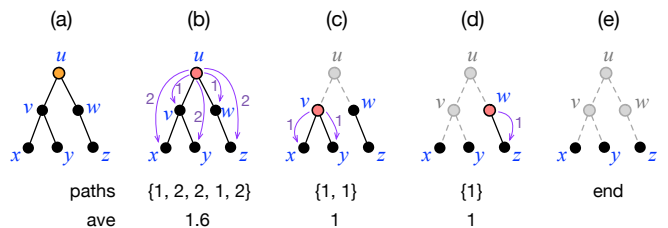


FIG. 3. Algorithm for quantifying cascade virality. To obtain the virality  $V_T$  of a tree  $T$ , we imagine the tree is rooted at node  $u$ . Once node  $u$  is removed, the tree would split into multiple subtrees (two subtrees in the given example), each rooted at one of  $u$ 's children (which are  $v$  and  $w$  in the case). Repeat the root node removal process step by step, until no more nodes have any descendants. Count the average path length between root nodes (which are  $u$ ,  $v$  and  $w$  in the case) and their descendants, then add them up immediately yields the desired  $V_T$ .

quantifies the average distance between any two nodes in a cascade tree, as the desired virality measure which they term *structural virality*. This attempt makes important advancement in quantitatively depicting the extent to which a cascade is viral, but it fails to account for the root of a cascade and inherently treats the cascade as an unrooted tree, thereby hindering its ability to differentiate cascades which are structurally different but will be considered as the same if the root nodes are neglected. (see Fig. 1 and Fig. 2). To remedy this and more precisely quantify the virality of cascades, we propose a root-aware approach. The obtained virality score is then named as *cascade virality*.

Specifically, the cascade virality of a rooted tree is quantified by the sum of the average path length between nodes and their descendants. Formally, for a rooted cascade tree  $T$  of size  $N$  ( $N \geq 2$ ), the cascade virality of  $T$  is

$$V_T = \sum_{i=1}^N \bar{d}_i, \quad (1)$$

where

$$\bar{d}_i = \sum_{j \in \mathcal{D}_i} d_{ij} / |\mathcal{D}_i|, \quad (2)$$

$d_{ij}$  denotes the distance from node  $i$  to one of its descendant  $j$ ,  $\mathcal{D}_i$  is the set of descendants of node  $i$  and  $|\bullet|$  represents the size of a set.

A schematic of the above process is shown in Fig. 3. Starting from the root node  $u$ , the average distance from node  $u$  to its descendants is counted, denoted as  $\bar{d}_u = ave(1, 2, 2, 1, 2) = 1.6$  (Fig. 3(b)); Suppose that node  $u$  is then removed, thus resulting in two subtrees with node  $v$  and  $w$  (i.e., child nodes of node  $u$ ) act as new root nodes for each subtree; The average distance from node  $v$  and  $w$  to their descendants is then computed as  $\bar{d}_v = ave(1, 1) = 1$  (Fig. 3(c)) and  $\bar{d}_w = ave(1) = 1$

	(a)	(b)	(c)	(d)	(e)	(f)	(g)	(h)	(i)
Cascades of size 5									
Wiener index	1.6	1.8	1.8	1.6	2.0	2.0	1.8	1.8	2.0
Cascade virality	1.0	2.25	2.5	2.75	3.5	4.25	4.33	4.92	7.0

FIG. 4. Cascades with five nodes and the corresponding Wiener index and cascade virality scores (shown below each cascade). Root nodes in each cascade are colored in orange. For Wiener index, equal values are shown in the same color.

(Fig. 3(d)); Repeat the above node removal and average path length calculation process, until no more nodes have descendants (Fig. 3(e)). The cascade virality of  $T$ ,  $V_T$ , is finally obtained by the sum over all the calculated average path length  $\bar{d}$ , which is  $\bar{d}_u + \bar{d}_v + \bar{d}_w = 3.6$  in the given example (Fig. 3). Also note that the proposed approach to quantifying the cascade virality of a rooted tree is easy to implement in a recursive manner, which enables the time complexity in the actual execution. A Python implementation of the algorithm is freely available online[23].

Fig. 4 presents direct comparisons between Wiener index and cascade virality for cascades with five nodes. As we can see from the figure, Wiener index, which quantifies the average distance between all pairs of nodes in a cascade tree, fails to distinguish several cascades as this virality measure doesn't take the root nodes into account. For instance, cascades in Fig. 4(e), 4(f) and 4(i) hold the same value in the context of Wiener index. Similar conditions can also be found for cascades in Fig. 4(a) and 4(d) as well as cascades in Fig. 4(b), 4(c), 4(g) and 4(h). In contrast, cascade virality is able to distinguish all the nine cascades in this scenario (last row in Fig. 4). Fig. 5 further illustrates cascades with six nodes and the corresponding values quantified by Wiener index and cascade virality. Compared with Fig. 4, Fig. 5 demonstrates that there are even more cascades that Wiener index fails to distinguish from each other. Specifically, for the twenty cascades illustrated in Fig. 5, only six virality scores are obtained under Wiener index. In contrast, cascade virality provides improved ability to distinguish different types of cascades. In other words, not considering the root node in a cascade tree has largely limited the expressive power of Wiener index in capturing the virality of cascades. It's expected that with the increase of cascade size, the ambiguities between cascades will become more and more severe under Wiener index. However, cascade virality, which considers the direction of the cascade flow, will be able to largely avoid these ambiguities compared with Wiener index.

The obtained cascade virality has good properties as well. For totally broadcast cascade (e.g., Fig. 4(a)), the virality is minimized and should be 1, as the root node directly connects all other nodes. For totally viral cascade of size  $N$  (e.g., Fig. 4(i)), the virality is maximized

and should be  $(N-1)(N+2)/4$  as the cascade tree is ultimately a path graph with the root node located at one end. For any other type of cascade, its virality is within the range  $[1, (N-1)(N+2)/4]$ . It's also anticipated that, for cascades with a fixed size, those with more generations (i.e., depths) are generally more viral than their counterparts with smaller generations. For example, as shown in Fig. 4, cascades with a depth of 3 (Fig. 4 (f)-(h)) are generally more viral than cascades with a depth of 2 (Fig. 4 (b)-(e)) and the cascade with a depth of 1 (Fig. 4 (a)).

## B. Application on empirical cascades

### 1. Virus strains

We first apply cascade virality on the phylogeny of virus strains. Fig. 6 shows the phylogenetic tree of two viruses—one is the ongoing novel coronavirus (SARS-CoV-2) in the region of Asia (denoted as SARS-CoV-2/Asia) and the other is the influenza H1N1pdm (denoted as flu/H1N1pdm)—obtained from Nextstrain [11]. Note that the leaf nodes represent the sampled strains, while the rest of nodes represent inferred common ancestors, and edges indicate the evolutionary relationships [11, 24].

Intuitively, flu/H1N1pdm tends to evolve in a more viral way than SARS-CoV-2/Asia. In fact, the quantified virality of flu/H1N1pdm cascade (with 3769 nodes and 65 generations) is 5021.89, while the quantified virality of SARS-CoV-2/Asia cascade (with 3431 nodes and 30 generations) is 3635.84. More detailed descriptions of evolutionary cascades of SARS-CoV-2 in six continents and four kinds of influenza viruses are further shown in Table I[25]. Based on the obtained data, we find that flu strains evolve into more generations than currently available SARS-CoV-2 strains since three out of four flu cascades go beyond the depth of 60 but no regional cascades of SARS-CoV-2 do so in current stage. Except for two large SARS-CoV-2 cascades in Europe and North America, the rest of SARS-CoV-2 cascades seem less viral than

virus	size	depth	virality
SARS-CoV-2/Africa	2646	37	2888.97
SARS-CoV-2/Asia	3431	30	3635.84
SARS-CoV-2/Europe	8241	51	8379.32
SARS-CoV-2/N. America	6309	42	6057.99
SARS-CoV-2/Oceania	3833	36	3895.62
SARS-CoV-2/S. America	2696	34	2847.81
flu/H1N1pdm	3769	65	5021.89
flu/H3N2	3826	71	6592.46
flu/Victoria	3140	66	3827.23
flu/Yamagata	2654	48	2877.85

TABLE I. Quantifying cascade virality on the phylogeny of virus strains.

	(a1-a2)		(b1-b4)				(c1-c2)		(d1-d4)				(e1-e5)					(f1-f3)		
Cascades of size 6																				
Wiener index	1.667		1.867				1.933		2.067				2.133					2.333		
Cascade virality	1	2.8	2.2	2.6	4.25	5.15	2.4	4.7	3.4	4.133	5.7	6.933	3.6	4.1	4.667	6.65	7.717	5.3	6.7	10

FIG. 5. Cascades with six nodes and the corresponding Wiener index and cascade virality scores.

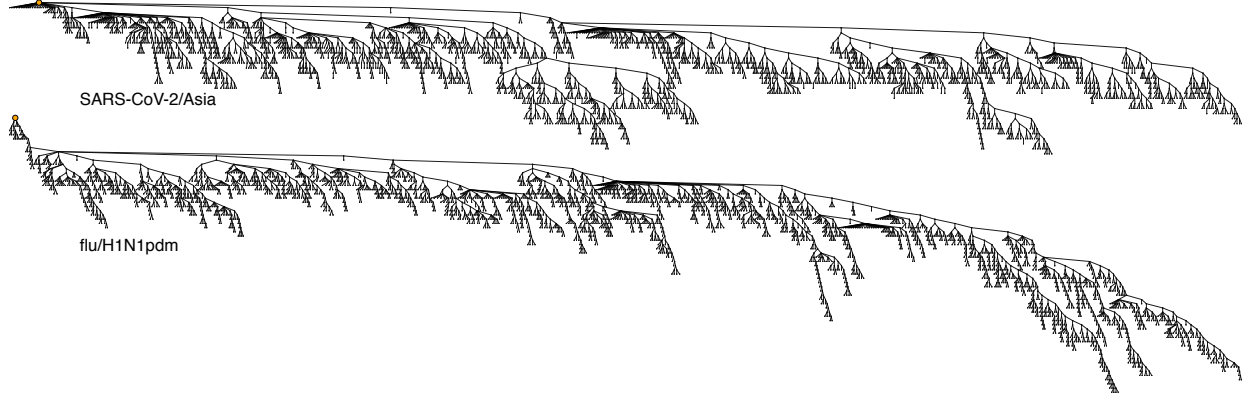


FIG. 6. Cascades of virus evolution. The upper and lower diagrams show the sampled genomic epidemiology of SARS-CoV-2 in Asia and the influenza H1N1pdm, respectively.

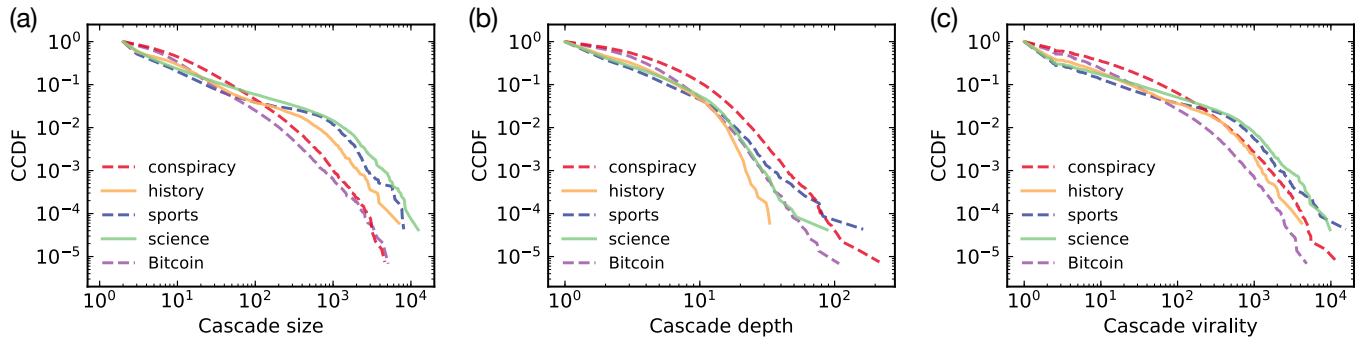


FIG. 7. Analysis of discussion cascades. (a) CCDF (Complementary Cumulative Distribution Function) of cascade size. (b) CCDF of cascade depth. (c) CCDF of cascade virality.

flu cascades. Nevertheless, it's foreseeable that the virality of SARS-CoV-2 cascades would increase dramatically in future if the rapid proliferation of SARS-CoV-2 is still out of control around the globe.

## 2. Discussion cascades

The obtained cascades of virus strains can be considered as very rare events, we then apply cascade virality on very general cases with large-scale online discussion data as examples. A discussion thread can be structurally represented as a rooted cascade tree, where the root node

denotes the post itself while each other nodes denotes a comment under this thread [21]. Leveraging discussion cascade data from five online communities in Reddit—a social news aggregation and discussion website—we conduct an analysis of cascade virality and its relation with cascade size and depth.

The dataset includes discussion cascades in five online domains, namely r/conspiracy, r/history, r/sports, r/science and r/Bitcoin, in the year of 2017 [26]. There are 344 396 cascades in total, including 133 917 in conspiracy, 16 741 in history, 23 178 in sports, 23 871 in science and 146 689 in Bitcoin. The CCDFs (Complementary Cumulative Distribution Functions) of cascade

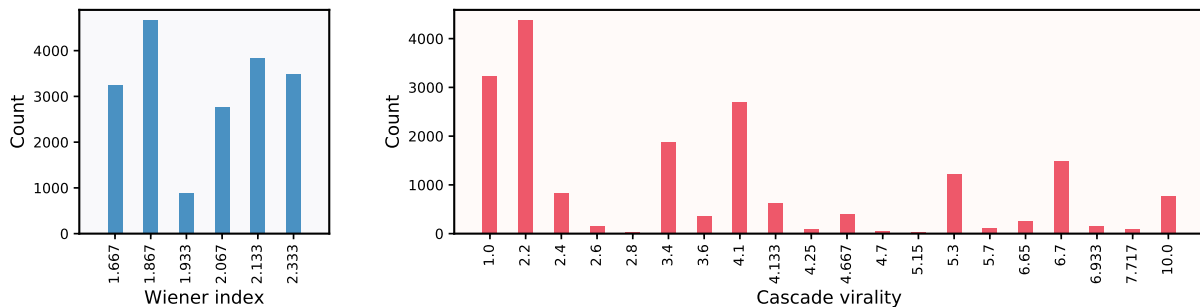


FIG. 8. Distributions of Wiener index and cascade virality for discussion cascades with 6 nodes. There are 18865 such cascades in total from the Reddit discussion data. Each bar corresponds to the count of cascades at specific virality scores under Wiener index or cascade virality.

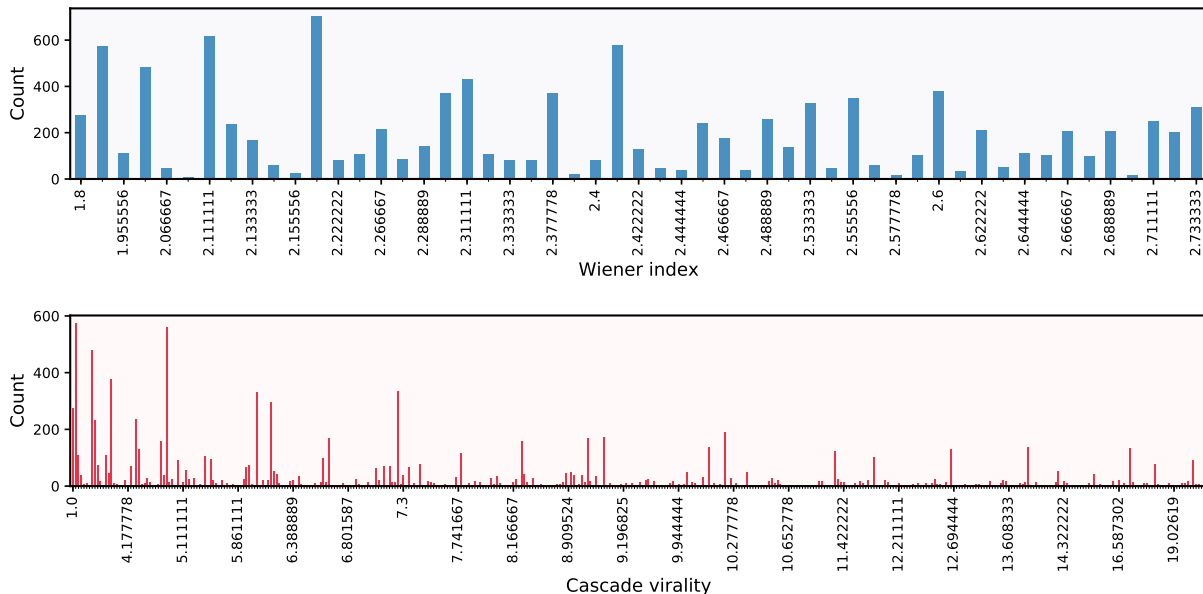


FIG. 9. Distributions of Wiener index and cascade virality for discussion cascades with 10 nodes. There are 10141 such cascades in total from the Reddit discussion data. Each bar corresponds to the count of cascades at specific virality scores under Wiener index or cascade virality.

size, depth and virality are shown in Fig. 7. As we can see from the figure, most of the cascades have a size of less than 100 (Fig. 7(a)) and a depth of less than 10 (Fig. 7(b)) across domains. We also note that conspiracy cascades are generally more viral than other kinds of cascades like science and sports (Fig. 7(c)).

Utilizing these empirical discussion cascades, we empirically evaluate the performances of Wiener index and cascade virality in characterizing the virality of cascades. For cascades with 6 nodes, Fig. 8 illustrates the number of cascades located at each virality scores under Wiener index (shown in blue) and cascade virality (shown in red). As shown in the figure, cascades are distributed on six Wiener index scores and twenty cascade virality scores. The disparities between the distributions of Wiener index and cascade virality become even clear for discussion cascades with 10 nodes (Fig. 9). Specifically, Wiener index results in 53 virality scores, but cascade virality is

able to quantify 412 levels of virality scores for the same set of cascade data.

To quantify such disparities between Wiener index and cascade virality described above, we conduct an entropy analysis for cascades with equal size. Given a set of cascades with  $N$  nodes, with possible virality scores  $v_i$ , each with probability  $P(v_i)$ , entropy of the virality score distribution is defined as follows:

$$H_N = - \sum_i P(v_i) \ln P(v_i). \quad (3)$$

For discussion cascades with equal size, we obtain an entropy for Wiener index and another for cascade virality. Fig. 11 shows the comparisons between Wiener index and cascade virality with the discussion cascade size increasing from 2 to 20. For discussion cascades with 2 nodes, the obtained entropy values via Wiener index and

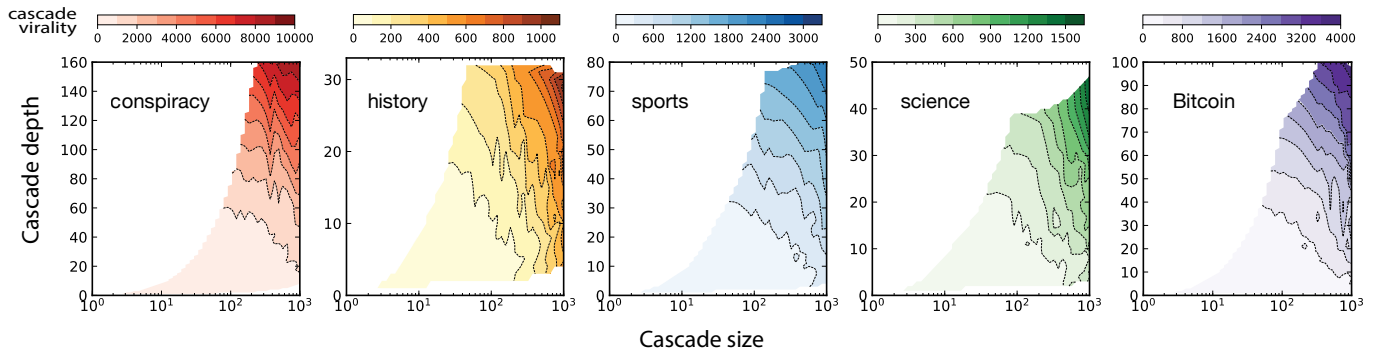


FIG. 10. Contour plots of cascade virality versus cascade size and depth. Color areas in each panel represent cascade virality scores in each domain, and darker regions indicate higher cascade virality scores. The contours are obtained by interpolating the data to regular grids using unstructured triangular grid functions from *Matplotlib*. Blank areas indicate no data available at specific points after the interpolation. For ease of visualization, contour lines are set as 10 levels for each domain.

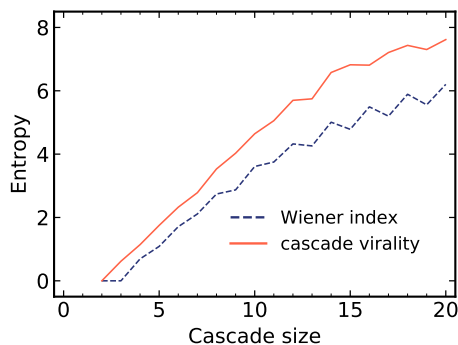


FIG. 11. Entropy analysis based on discussion cascades from Reddit.

cascade virality show no differences as both of them are equal to 0 in this scenario. For discussion cascades with 3 nodes, Wiener index will output a unique virality score as it doesn't consider the positions of the root nodes, but cascade virality is able to disambiguate cascades with the root node located at one end and cascades with the root node located at the center (see Fig. 2 for detailed illustrations). Therefore, we find a higher entropy of cascade virality than that of Wiener index for cascades with 3 nodes in Fig. 11. And more importantly, for increasing cascade size, we find that cascade virality consistently outperforms Wiener index according to the entropy analysis on empirical cascades (Fig. 11). Based on the above illustrated cascade examples and analyses, it's becoming clear that without considering the root nodes, Wiener index is not adequate to characterize the virality of cascades, as many cascades will be deemed as the same if the root node is neglected. However, cascade virality, which takes the root node into account, can largely disambiguate cascades that Wiener index has failed to do so.

With a further exploration of empirical discussion data, we find that both cascade size and depth empirically contribute to an increase of cascade virality across

domains (Fig. 10). As shown in Fig. 10, cascade virality scores become larger and larger from the lower left to the upper right of the graph in each subplot [27]. In other words, for cascades with equal sizes, those whose depths are deeper tend to have higher cascade virality scores. Likewise, for cascades with equal depths, those whose sizes are larger are also more likely to have higher cascade virality scores. In summary, in light of the discussion cascades from five online domains, we find empirical evidence that cascade virality is positively correlated with both cascade size and depth.

### III. MODELING CASCADE GROWTH

Preferential attachment, especially for Barabási-Albert (BA) preferential attachment, has been widely adopted to model the growth of complex networks [17–19, 24, 28–32]. Specifically, it assumes that, at each time step, the probability that an incoming node added to node  $i$  is proportional to node  $i$ 's degree  $k_i$  in the network. More generally, one might consider a non-linear attachment kernel, where the attachment is proportional to node's degree raised to the power  $\gamma$ ,

$$p_i = \frac{k_i^\gamma}{\sum_j k_j^\gamma}, \quad (4)$$

where  $k_j$  denotes the degree of node  $j$  and the sum is over all nodes already present in the network, and the parameter  $\gamma$  controls the attachment intensity.

As one special case of complex network, a tree-structure network is achieved when each new node only connects to one (instead of multiple) existing node [18]. Recalling the way we quantify cascade virality, it's anticipated that during the growth of a cascade, new node attachment to long-range leaf nodes would result in a more viral cascade than the attachment to nodes that are close to the root node (Fig. 12(a)). To mimic the growth of cascades and particularly control the virality of cascades

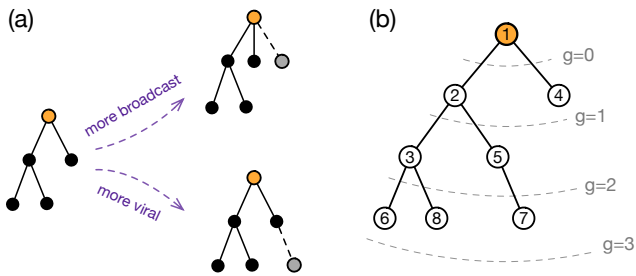


FIG. 12. (a) Schematic of broadcast versus viral growth. (b) Genealogy of a cascade tree. Root node is shown in color, and dashed lines indicate different genealogy levels of the root node (node 1).

during the growth process, we propose a genealogy-based preferential attachment mechanism inspired by classical degree-based attachment kernel. We will illuminate the proposed model in detail below.

### A. Cascade growth based on network genealogy

For a cascade tree, once the root node is determined, its genealogy is readily available. Note that, for any node in a cascade tree, its genealogy can be represented by a (sub)tree rooted at itself.

Fig. 12(b) illustrates such an example tree rooted at node 1, where the genealogy levels of node 1 are denoted by  $g$ . Specifically, nodes 2-8 are all descendants of node 1, resulting in a genealogy of size 8 for node 1 (including node 1 itself), while only nodes 3 and 5-8 are node 2's descendants in the rooted tree, thus resulting in a genealogy of size 6 for node 2 (including node 2 itself). More importantly, the genealogy of node 1 at level 1 includes nodes 1, 2 and 4, resulting in a genealogy of size 3 at this level; while the genealogy at level 2 includes two more nodes (nodes 3 and 5), suggesting a genealogy of size 5 at this level. Similarly, for genealogy of node 2, there are three nodes (nodes 2, 3 and 5) at level 1 and six nodes (nodes 2, 3 and 5-8) at level 2.

Formally, for node  $i$  in a cascade tree, its complete genealogy contains itself and all the descendants of it, but the genealogy at level  $g$  contains itself and its descendants within  $g$  generations only. For the sake of consistency, the complete genealogy is also denoted as genealogy at level  $max$ .

Here, we propose a genealogy-based preferential attachment model, where new node attachment relies on a node's genealogy size at specific genealogy levels instead of degree. Namely,

$$p_i = \frac{d_{ig}^\gamma}{\sum_j d_{jg}^\gamma}, \quad (5)$$

where  $d_{jg}$  is the genealogy size of node  $j$  at level  $g$ , and the parameter  $\gamma$  controls the attachment intensity.

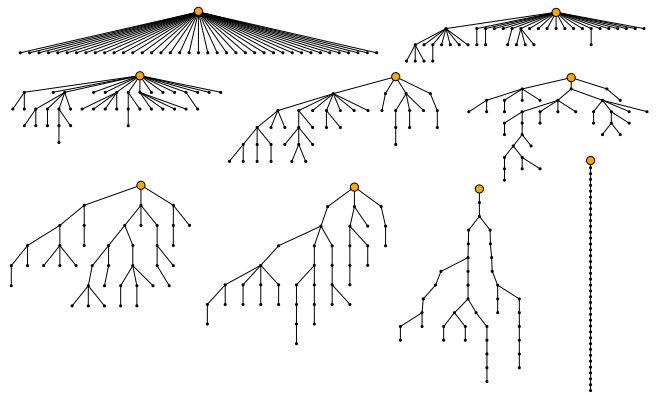


FIG. 13. Synthetic cascades when the complete genealogy is considered in the attachment kernel with  $\gamma \in \{5.0, 1.5, 0.75, 0.25, 0, -0.25, -1.0, -2.5, -10.0\}$  (from top left to bottom right). Taking cascades of size 40 for illustration purposes only.

Clearly,  $\gamma = 1$  recovers the linear attachment kernel while  $\gamma = 0$  recovers the uniform attachment kernel. When  $\gamma > 1$ , the attachment kernel becomes super-linear, while in the interval  $0 < \gamma < 1$ , the attachment kernel becomes sub-linear. For  $\gamma < 0$ , the model favors homogeneous attachment where incoming nodes are preferentially attached to existing nodes with small genealogy sizes.

It's anticipated that in the limit  $\gamma \rightarrow +\infty$ , the model would generate totally broadcast cascade trees, where the root node directly connects all other nodes. In the limit  $\gamma \rightarrow -\infty$ , the model would generate totally viral cascade trees, where each node has one successor only except for the last node which acts as the leaf node.

### B. Numerical results on synthetic cascades

We numerically evaluate the effect of parameter  $\gamma$  in driving the virality of cascades. Fig. 13 shows the generated cascades based on complete genealogy with the varying  $\gamma \in \{5.0, 1.5, 0.75, 0.25, 0, -0.25, -1.0, -2.5, -10.0\}$  when the cascade size is set as 40. As shown in the figure, for  $\gamma > 1$ , the generated cascades tend to condense on nodes at low depths (particularly on the root node), where the number of successors diminishes with the increase of distance from the root node. When  $\gamma$  is set by large positive values, such as 5.0 in the example, the generated cascade will condense completely on the root node, which corresponds to a totally broadcast cascade. With the decrease of  $\gamma$ , the condensation state diminishes gradually and even becomes trivial for negative values of  $\gamma$ . When  $\gamma$  is set by negative values with large magnitude, such as -10 in the given example, the generated cascade will form a long path with the root node located at one end, which corresponds to a totally viral cascade.

Further, we numerically investigate the relationship between cascade virality and parameter  $\gamma$  in different cas-

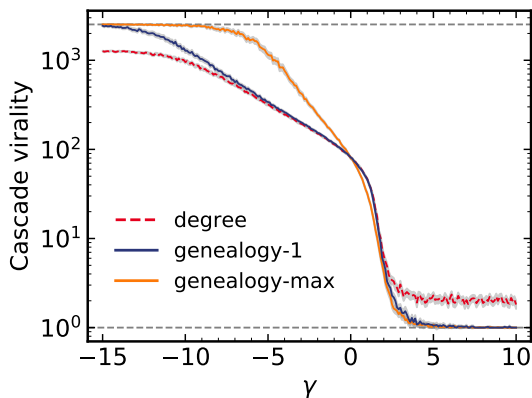


FIG. 14. Cascade virality versus parameter  $\gamma$  according to different growth mechanisms (using cascades of size 100 for illustration). Cascade virality bounds are shown in grey dashed horizontal lines. Shading areas (in grey) indicate bootstrapped 95% confidence intervals obtained from 100 random simulations under each parameter  $\gamma$ . As shown in the figure, classic degree-based mechanism cannot efficiently exhaust the complete virality space.

cade growth models. We consider not only the complete genealogy size but also genealogy at level 1 and classic degree based attachment kernel. Specifically, cascade size is set as 100,  $\gamma$  is set in the range of  $[-15, 10]$  with a step of 0.1, and 100 cascades are generated under parameter  $\gamma$  in each growth model.

In Fig. 14, we show the cascade virality for increasing  $\gamma$ . Note that, for cascades of size 100, their virality scores are located within the range  $[1, 2524.5]$ . The upper and lower bounds are shown in grey dashed horizontal lines in the figure. Clearly, cascade virality decreases with the increase of parameter  $\gamma$  in each model, but classic degree-based kernel cannot efficiently exhaust the complete virality space. With the increase of  $\gamma$ , two genealogy-based models ultimately converge to completely condensate state, which is not observed for degree-based kernel. In summary, genealogy-based models provide much more strong representation power than classic degree-based model in generating cascades with varying virality scores.

### C. Numerical results on empirical cascades

We test the performance of cascade growth models on empirical discussion cascades described above. For each discussion cascade, a synthetic cascade with the same size is generated according to each growth model. We then compare the virality of generated cascades with that of real cascades in terms of the distribution of virality scores. The comparison can be done by Kolmogorov-Smirnov (KS) statistic between the generated cascade virality scores and real cascade virality scores.

The KS statistic of two distributions is given by the maximum discrepancy between their cumulative distri-

bution functions (CDFs), and has been applied in assessing the goodness of fit between two degree distributions [24, 33]. Generally, smaller KS statistic favors better fit. Given the empirical virality distribution, we estimate  $\gamma$  by minimizing the KS statistic averaged over ten random simulations under each parameter  $\gamma$ . The optimal  $\gamma$  for each model under each community is chosen as the  $\gamma$  that results in the minimum KS statistic over the parameter space.

For ease of computation, cascades whose sizes are larger than 100 or the 95th percentile, whichever is greater, are omitted in the analysis. Cascades of size 2 are also not included as any cascade growth model can exactly generate the same kind of cascade with 2 nodes. Fig. 15 presents the results for degree, genealogy-1 and genealogy-max based models, where smaller minimum KS statistic indicates better model under each community.

As shown in the figure, the minimum KS statistics achieved by degree-based model are larger than 0.097 across all five domains, while genealogy-based models show better performance with the minimum KS statistics all less than 0.096 (see also Table II for details). Specifically, genealogy-1 achieves better performance than genealogy-max. In summary, leveraging data of discussion cascades from five online domains, we demonstrate the performance of genealogy-based models to mimic the growth of cascades.

TABLE II. The minimum KS statistic for each model.

	conspiracy	history	sports	science	Bitcoin
degree	0.098	0.121	0.134	0.167	0.108
genealogy-1	0.083	0.078	0.070	0.074	0.080
genealogy-max	0.089	0.095	0.088	0.090	0.092

## IV. CONCLUSION

In this work, we introduce a root-aware approach to quantifying the virality of cascades. The proposed approach considers cascades as directed instead of undirected trees, thus alleviating the effects induced by graph isomorphism that previous studies have overlooked. Using synthetic and empirical cascades, we show the property and utility of the proposed approach and particularly the relationships between cascade virality and cascade size and depth. In doing so, we find that both cascade size and depth empirically contribute to an increase of cascade virality from the obtained large-scale discussion data.

To mimic the growth of cascades as an interpolation between broadcast and viral proliferation, we further introduce a cascade growth model. Specifically, the attachment kernel is constructed based on node genealogy rather than node degree. With the decrease of the attachment intensity, the generated cascade grows from



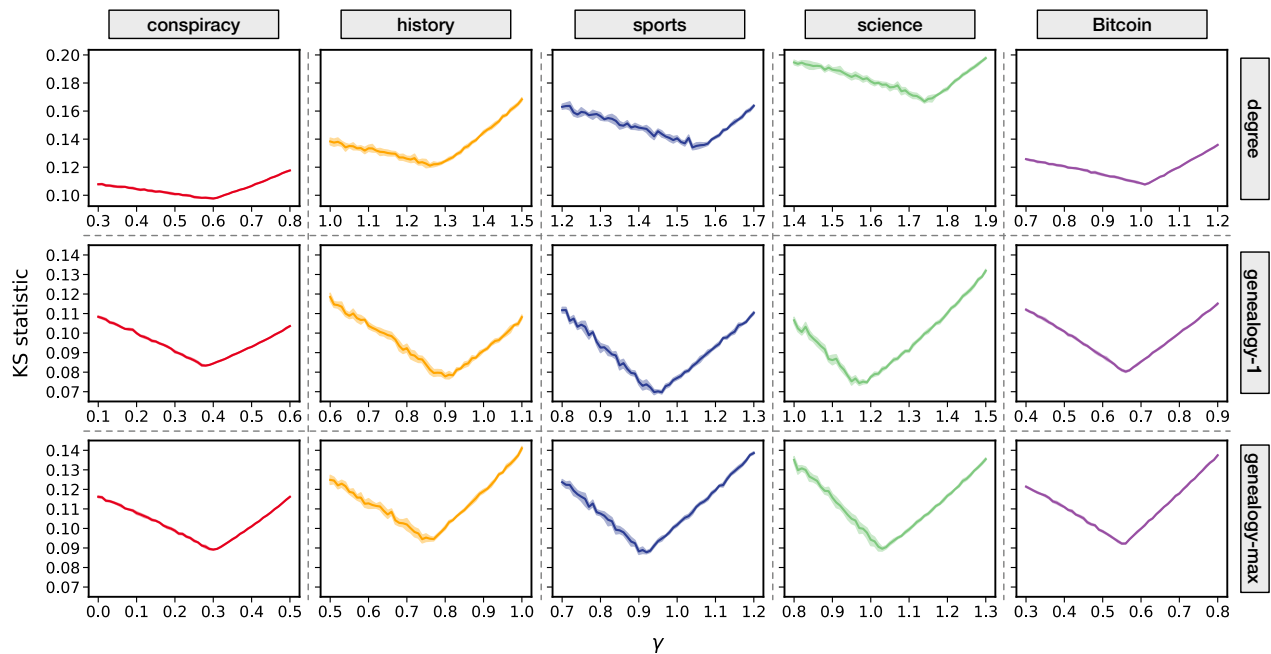


FIG. 15. KS-statistic versus parameter  $\gamma$  in numerical simulations. KS-statistic measures the maximum discrepancy between the cumulative distribution functions (CDFs) of two virality distributions: the empirical virality distribution and the generated virality distribution. Shading areas indicate bootstrapped 95% confidence intervals obtained from ten random simulations.

a broadcast to a viral way. Numerical simulations on synthetic and empirical cascades reveal the advantage of genealogy-based attachment kernel over degree-based attachment kernel in characterizing the virality of cascades.

Our work contributes to a further understanding of how to quantify the virality of cascades and provides a rich avenue for compelling applications. For example, as we have demonstrated in the main text, conspiracy and science cascades display quite different patterns in the distribution of cascade virality. As such, the proposed approach to quantifying cascade virality may provide improved ability to distinguish different types of cascades. Moreover, as shown in the paper, the attachment kernel significantly affects the growth and virality of cascades, which may offer valuable insights to the implementation of viral marketing in practice. In this work, we mainly address tree-structure cascades, but future works may consider more complex diffusion structures, such as the locally tree-like diffusion process which is prevalent in network spreading. We have applied the proposed measure to capture the virality of SARS-CoV-2 and influenza strains, but future works can directly apply it on infection data (once such data are available) to have a better understanding of the spread of virus.

## Appendix A: Property

For a cascade  $T$  of size  $N$  ( $N \geq 2$ ), the cascade virality of it satisfies the following:  $1 \leq V_T \leq (N-1)(N+2)/4$ .

1. Extreme case when the cascade virality is minimized: a star graph with the root located at the hub (i.e., totally broadcast), and the corresponding virality of the cascade is  $V_T = 1$ ;
2. Extreme case when the cascade virality is maximized: a path graph with the root located at one end (i.e., totally viral)

- For a complete path cascade  $T$  of size 2, the cascade virality is 1;
- For a complete path cascade  $T$  of size  $N$  ( $N \geq 3$ ), the cascade virality is  $V_T = 1 + \frac{1+2}{2} + \dots + \frac{1+2+\dots+(N-1)}{N-1} = 1 + \frac{3}{2} + \dots + \frac{N}{2} = \frac{2+3+\dots+N}{2} = \frac{(N-1)(N+2)}{4}$ ;

Taken together, we know that for a complete path cascade  $T$  of size  $N$ , its cascade virality is  $V_T = \frac{(N-1)(N+2)}{4}$ .

Therefore, for a cascade  $T$  of size  $N$  ( $N \geq 2$ ), the cascade virality of it should lie between 1 and  $(N-1)(N+2)/4$ .

- 
- [1] S. Goel, A. Anderson, J. Hofman, and D. J. Watts, *Management Science* **62**, 180 (2015).
- [2] S. Vosoughi, D. Roy, and S. Aral, *Science* **359**, 1146 (2018).
- [3] J. Cheng, L. Adamic, P. A. Dow, J. Kleinberg, and J. Leskovec, in *Proceedings of the 23rd international conference on World wide web* (ACM, 2014) pp. 925–936.
- [4] D. Liben-Nowell and J. Kleinberg, *Proceedings of the National Academy of Sciences* **105**, 4633 (2008).
- [5] H. Liang, *Journal of Communication* **68**, 525 (2018).
- [6] R. Kumar, M. Mahdian, and M. McGlohon, in *Proceedings of the 16th ACM SIGKDD international conference on Knowledge Discovery and Data Mining* (ACM, 2010) pp. 553–562.
- [7] V. Gómez, H. J. Kappen, and A. Kaltenbrunner, in *Proceedings of the 22nd ACM conference on Hypertext and Hypermedia* (ACM, 2011) pp. 181–190.
- [8] A. N. Medvedev, J.-C. Delvenne, and R. Lambiotte, *Journal of Complex Networks* **7**, 67 (2018).
- [9] R. Pastor-Satorras, C. Castellano, P. Van Mieghem, and A. Vespignani, *Reviews of Modern Physics* **87**, 925 (2015).
- [10] S. Ferreira Jr, M. Martins, and M. Vilela, *Physical Review E* **65**, 021907 (2002).
- [11] J. Hadfield, C. Megill, S. M. Bell, J. Huddleston, B. Potter, C. Callender, P. Sagulenko, T. Bedford, and R. A. Neher, *Bioinformatics* **34**, 4121 (2018).
- [12] A. Moinet, R. Pastor-Satorras, and A. Barrat, *Physical Review E* **97**, 012313 (2018).
- [13] A. Anderson, D. Huttenlocher, J. Kleinberg, J. Leskovec, and M. Tiwari, in *Proceedings of the 24th international conference on World Wide Web* (ACM, 2015) pp. 66–76.
- [14] A. Banerjee, A. G. Chandrasekhar, E. Duflo, and M. O. Jackson, *Science* **341**, 1236498 (2013).
- [15] J. L. Iribarren and E. Moro, *Physical Review E* **84**, 046116 (2011).
- [16] L. Zhang and T.-Q. Peng, *Internet Research* **25**, 453 (2015).
- [17] A.-L. Barabási and R. Albert, *Science* **286**, 509 (1999).
- [18] P. L. Krapivsky, S. Redner, and F. Leyvraz, *Physical Review Letters* **85**, 4629 (2000).
- [19] P. L. Krapivsky and S. Redner, *Physical Review E* **63**, 066123 (2001).
- [20] Q. Zhao, M. A. Erdogdu, H. Y. He, A. Rajaraman, and J. Leskovec, in *Proceedings of the 21th ACM SIGKDD international conference on Knowledge Discovery and Data Mining* (ACM, 2015) pp. 1513–1522.
- [21] R. Krohn and T. Wenering, arXiv preprint arXiv:1910.08575 (2019).
- [22] J. Overgoor, A. Benson, and J. Ugander, in *The World Wide Web Conference* (ACM, 2019) pp. 1409–1420.
- [23] [https://github.com/yflyzhang/cascade\\_virality](https://github.com/yflyzhang/cascade_virality).
- [24] J.-G. Young, G. St-Onge, E. Laurence, C. Murphy, L. Hébert-Dufresne, and P. Desrosiers, *Physical Review X* **9**, 041056 (2019).
- [25] The raw genomic epidemiology data are acquired from and publicly available at <https://nextstrain.org>. Accessed: 2020-04-29.
- [26] The raw data of Reddit are acquired from and publicly available at <https://files.pushshift.io/reddit>.
- [27] The contours are obtained using tools from *Matplotlib*: [https://matplotlib.org/3.1.1/api/tri\\_api.html](https://matplotlib.org/3.1.1/api/tri_api.html).
- [28] M. Golosovsky, *Physical Review E* **97**, 062310 (2018).
- [29] M. E. Newman, *Physical Review E* **64**, 025102 (2001).
- [30] H. Jeong, Z. Néda, and A.-L. Barabási, *EPL (Europhysics Letters)* **61**, 567 (2003).
- [31] E. Eisenberg and E. Y. Levanon, *Physical Review Letters* **91**, 138701 (2003).
- [32] A. Capocci, V. D. Servedio, F. Colaiori, L. S. Buriol, D. Donato, S. Leonardi, and G. Caldarelli, *Physical Review E* **74**, 036116 (2006).
- [33] A. Clauset, C. R. Shalizi, and M. E. Newman, *SIAM review* **51**, 661 (2009).